Characterisation of Asp669Tyr Piezo1 cation channel activity in red blood cells: an unexpected phenotype

Laurent Pérès, David Monedero Alonso, Morgane Nudel, Martin Figeac, Judith Bruge, Shéhérazade Sebda, Veronique Picard, Wassim El Nemer, Claude Preudhomme, Christian Rose, et al.

Characterization of Asp669Tyr Piezo1 cation channel activity in red blood cells: an unexpected phenotype

Laurent Pérès[1,7*], David Monedero Alonso[1,7*], Morgane Nudel[2], Martin Figeac[3,4], Judith Bruge[2], Shéhérazade Sebda[3], Véronique Picard[5], Wassim El Nemer[6,7], Claude Preudhomme[3], Christian Rose[2†], Stéphane Egée[1,7#], Guillaume Bouyer[1,7#$]

[1] Sorbonne Université, CNRS, UMR8227, Station Biologique de Roscoff, France

[2] Hôpital Saint Vincent de Paul, Université Catholique, F-59000 Lille, France

[3] Univ-Lille, Plate-forme de Génomique Fonctionnelle et Structurale, F-59000 Lille, France

[4] CHU Lille, cellule bioinformatique, plateau commun de séquençage, F-59000 Lille, France

[5] Hématologie biologique, CHU Bicêtre, Le Kremlin Bicêtre, France

[6] Inserm, UMR_S 1134, Institut National de la Transfusion Sanguine INTS, Paris, France

[7] Laboratoire d'Excellence GR-Ex, France

* Contributed equally to this work

# Contributed equally to this work

† Deceased

$ Corresponding author, email: bouyer@sb-roscoff.fr

Human red blood cells (RBCs) have a unique capacity to deformability linked to volume preservation via membrane permeability control. Most notably, defects in proper cation permeability maintenance is implicated in several diseases (1). Dehydrated Hereditary Stomatocytosis (DHS), also termed Hereditary Xerocytosis [Online Mendelian Inheritance in Man (OMIM®) 194380], is a rare autosomal dominant congenital haemolytic anaemia, characterized by decreased intracellular K^+ concentration, uncompensated by Na^+ increase. RBCs are dehydrated with resulting increased Mean Corpuscular Haemoglobin (Hb) Concentration (MCHC), and decreased osmotic fragility (1). Ektacytometry reveals a characteristic profile with normal Elongation Index (EI_{max}) and largely decreased O_{min} (osmolality at which EI reaches a minimum in the hypotonic region) and O_{hyper} (osmolality at 50% of EImax in the hypertonic region) (1). Mutations affecting two cation channels have been linked to the disease: Piezo1, a mechanosensitive non-selective cation channel (2) and Gárdos channel [potassium calcium-activated channel subfamily N member 4 (KCNN4)], a K^+ selective channel activated by intracellular Ca^{2+} (3,4). However, recent case report tend to discriminate Piezo1 and Gárdos channel-related pathologies (5). Multiple mutations on Piezo1 channel leading to DHS symptoms have been recently described (6,7), however functional characterization of mutant channels is often restricted to heterologous expression. Here we use complementary techniques to describe cation channel activity directly within RBCs of a patient harbouring a mutation (Piezo1 D669Y) previously associated to DHS but never functionally characterized.

The patient has been suffering from episodic haemolytic anaemia since he was 5 years old. Biological parameters measured so far indicate a Hb concentration of 114g/l, a Mean Corpuscular Volume (MCV) of 101fl, an MCHC of 350g/l. Circulating reticulocytes level was 177g/l (5.6%). Furthermore, this patient had a bilirubinemia of 20mg/l of which 17mg/l unbound. Etiological investigations conducted since early childhood had not provided any diagnosis, although an enhanced osmotic resistance and an increase of foetal haemoglobin up to 2.1% were observed.

The *de-novo* comparative study, by whole exome sequencing, of the two parents and of the *propositus,* revealed one *in-silico* predicted deleterious single anomaly: a heterozygous variation of the Piezo-type mechanosensitive ion channel component 1 (*PIEZO1*) gene present in exon 16 (NM_001142864.2:c.2005 G>T), leading to the mutation D669Y in the *propositus*. The same mutation was reported in two reports compiling data on large sets of DHS patients (6,7) and in a Portuguese patient displaying "sporadic" xerocytosis (ClinVar Accession VCV000829815.1); another variant on the same residue (D669H) with haemolytic anaemia has also been reported (8). Until now, these mutations lack functional characterization. The site is rather distal when compared to most mutations described so far and belongs to a highly conserved motif within one of the two putative extracellular domains responsible for mechanotransduction described for mPiezo1 homologous channel (9) (supplementary fig. 1A-C).

On smears, Piezo1 D669Y RBCs displayed an enlarged projected area (fig. 1A), consistent with an increased deformability, and are slightly elliptocytic as confirmed by the decreased cell roundness (fig. 1B); multiple aberrant shapes were observed (supplementary fig. 1D). Ektacytometry revealed a mild DHS profile for D669Y Piezo1 RBCs (fig. 1C): O_{min} is reduced (increased osmotic resistance), EI_{max} is increased (increased deformability) and O_{hyper} is only slightly reduced (mild dehydration). This was confirmed by osmotic fragility curves (fig. 1D), and by measuring hydration and cation concentration status of RBCs. As expected, intracellular K^+ was decreased, but surprisingly intracellular Na^+ is increased and cell water content is preserved (fig. 1E). Checking total intracellular cation content revealed that K^+ decreased content was nearly compensated by increased Na^+ (fig. 1F), an unusual feature for DHS. This raised two questions about the Na^+ entry pathway(s): (i) is it Piezo1 channel itself or another cation transporter regulated downstream? (ii) Is this linked to constant Na^+ small leakage into the cell, or to bursts of activity that Na^+/K^+ pump is unable to cope with?

Next we used carbonyl cyanide *m*-chlorophenylhydrazone (CCCP), a protonophore that allows monitoring of membrane potential of RBCs via extracellular pH measurement (10). We recently used this method to describe channel activity on RBCs either with KCNN4 or Piezo1 variants (5,11). The results unveil differences in cation channel activity of control and patient RBCs (detailed description in the supplementary section). Main conclusions are (i) that both resting membrane potential and Gárdos channel activity are not affected by the mutation (fig. 2A), and (ii) a greater Non Selective Cation channel activity can be observed that notably allows entry of Na^+ (fig. 2A-B). Since Piezo1 is also an entry pathway for Ca^{2+}, we monitored resting Ca^{2+} content using a calcium fluorescent probe (Fluo-4) as well as Ca^{2+} uptake susceptibility using Piezo1 channel activator Yoda-1 (fig. 2C). We observed that (i) basal Ca^{2+} content was significantly higher and (ii) Ca^{2+} uptake after Yoda-1 activation was magnified in *propositus* RBCs, suggesting either an enhanced susceptibility of Piezo1 channel to Yoda-1, or an increased maximal activity of the channel. Altogether, these results show that non-selective cation channel activity is enhanced in patient RBCs and can provide a route for Na^+ and Ca^{2+} entry, likely via Piezo1 channel activity. Normal $[Ca^{2+}]_i$ of RBCs is kept below 50nM (12), a small increase can be sufficient to activate transiently the Gárdos channel (EC_{50} 4.7µM) (13).

Finally, patch-clamp technique revealed an enhanced cation channel activity with an increased whole-cell conductance of D669Y Piezo1 RBCs (fig. 2D). When looking in details, only 4 out of 7 patient cells displayed a spontaneously increased channel activity (fig. 2E). This variability might be linked to cell age, and this hypothesis is strengthened by the established correlation between senescence, cell calcium (14) and Gárdos channel (15), pointing to an accelerated ageing in patient RBCs.

In conclusion, we used several complementary methods to characterize the consequences of the Piezo1 D669Y mutation that leads to an unusual DHS phenotype with surprisingly limited cell dehydration. We revealed a gain of function for the Piezo1 D669Y, providing a route not only for Ca^{2+} but also for Na^{+} to enter RBCs, compensating K^{+} loss. The mutation might decrease the lifespan of RBCs with sudden and more frequent activation of the Gárdos channel. This last assumption is underpinned by the heterogeneity of spontaneous currents recorded using patch-clamp, and by the diversity of cell shapes observed in smear analyses. More generally, such results illustrate the complexity of DHS RBC profiles, which likely depend on cell age.

Acknowledgement

We thank the patient and his family who gave informed written consent and generously provided blood samples for this study. This work is dedicated to the memory of Pr. Christian Rose, who followed the patient and initiated the collaboration between all groups.

Disclosures

The authors declare no relevant conflicts of interest. LP, DMA, WEN, GB and SE are supported by the Laboratory of Excellence Labex GR-Ex, reference ANR-11-LABX-0051; GR-Ex is funded by the program “Investissements d’avenir” of the French National Research Agency, reference ANR-11-IDEX-0005-02. DMA was supported by the European Union’s Horizon 2020 Research and Innovation Program under grant agreement No. 675115 – RELEVANCE – H2020-MSCA-ITN-2015/H2020-MSCA-ITN-2015.

Author contributions

CR, MF, VP, CP, SE and GB designed the study and supervised the study. LP, DMA, MN, MF, JB, SS, VP, WEL, CP, SE, GB performed research and data analysis. SE, GB wrote the manuscript and designed the figures. All authors revised the manuscript.

Bibliography

1. Andolfo I, Russo R, Gambale A, Iolascon A. New insights on hereditary erythrocyte membrane defects. Haematologica. 2016;101(11):1284‑94.

2. Zarychanski R, Schulz VP, Houston BL, Maksimova Y, Houston DS, Smith B, et al. Mutations in the mechanotransduction protein PIEZO1 are associated with hereditary xerocytosis. Blood. 2012;120(9):1908‑15.

3. Glogowska E, Lezon-Geyda K, Maksimova Y, Schulz VP, Gallagher PG. Mutations in the Gardos channel (KCNN4) are associated with hereditary xerocytosis. Blood. 2015;126(11):1281‑4.

4. Rapetti-Mauss R, Lacoste C, Picard V, Guitton C, Lombard E, Loosveld M, et al. A mutation in the Gardos channel is associated with hereditary xerocytosis. Blood. 2015;126(11):1273‑80.

5. Fermo E, Monedero-Alonso D, Petkova-Kirova P, Makhro A, Pérès L, Bouyer G, et al. Gardos channelopathy: functional analysis of a novel KCNN4 variant. Blood Adv. 2020;4(24):6336‑41.

6. Picard V, Guitton C, Thuret I, Rose C, Bendelac L, Ghazal K, et al. Clinical and biological features in PIEZO1-hereditary xerocytosis and Gardos-channelopathy: A retrospective series of 126 patients. Haematologica. 2019;haematol.2018.205328.

7. Andolfo I, Russo R, Rosato BE, Manna F, Gambale A, Brugnara C, et al. Genotype-phenotype correlation and risk stratification in a cohort of 123 hereditary stomatocytosis patients. Am J Hematol. 2018;93(12):1509‑17.

8. Maciak K, Adamowicz-Salach A, Siwicka A, Poznanski J, Urasinski T, Plochocka D, et al. Hereditary xerocytosis - spectrum and clinical manifestations of variants in the PIEZO1 gene, including co-occurrence with a novel β-globin mutation. Blood Cells Mol Dis. 2020;80:102378.

9. Zhao Q, Zhou H, Li X, Xiao B. The mechanosensitive Piezo1 channel: a three-bladed propeller-like structure and a lever-like mechanogating mechanism. FEBS J. 2019;286(13):2461‑70.

10. Macey RI, Adorante JS, Orme FW. Erythrocyte membrane potentials determined by hydrogen ion distribution. Biochim Biophys Acta. 1978;512(2):284‑95.

11. Filser M, Giansily-Blaizot M, Grenier M, Monedero Alonso D, Bouyer G, Peres L, et al. Increased incidence of germline PIEZO1 mutations in individuals with idiopathic erythrocytosis. Blood [Internet]. 2020;(blood.2020008424). https://doi.org/10.1182/blood.2020008424

12. Lew VL, Tsien RY, Miner C, Bookchin RM. Physiological $[Ca^{2+}]i$ level and pump-leak turnover in intact red cells measured using an incorporated Ca chelator. Nature. 1982;298(5873):478‑81.

13. Leinders T, van Kleef RG, Vijverberg HP. Single Ca(2+)-activated K+ channels in human erythrocytes: Ca^{2+} dependence of opening frequency but not of open lifetimes. Biochim Biophys Acta. 1992;1112(1):67-74.

14. Lew VL, Tiffert T. On the Mechanism of Human Red Blood Cell Longevity: Roles of Calcium, the Sodium Pump, PIEZO1, and Gardos Channels. Front Physiol. 2017;8(977).

15. Klei TRL, Dalimot JJ, Beuger BM, Veldthuis M, Ichou FA, Verkuijlen PJJH, et al. The Gardos effect drives erythrocyte senescence and leads to Lu/BCAM and CD44 adhesion molecule activation. Blood Adv. 2020;4(24):6218‑29.

Figure legend

Figure 1. Morphological parameters and ionic status of D669Y Piezo1 RBCs.

(A-B) Distribution of cell projected area (A) and cell roundness (B) from control (blue) and patient (red) RBCs, measured from peripheral blood smears and quantified using Fiji. n>1000 cells for both cell types. Cell roundness is defined as $4x[Area]/\pi\times[Major\ axis]^2$. (C) Ektacytometry profile of patient (red) and control (blue) RBCs. Dots indicate O_{min}, EI_{max} and O_{hyper}. (D) Osmotic fragility curves for patient (red) and control (blue) RBCs. (E) Cell content in water (left), Na^+ (middle) and K^+ (right) of control (blue) and patient (red) RBCs. Patient intracellular K^+ [100.7±1.8 mmol/litre cell water (lcw)] is lower than control (125.6±12.7 mmol/lcw), p=0.1), whereas intracellular Na^+ is increased (27.7±12.2 vs 13.7±3.1 mmol/lcw, p=0.1). Cell water content is preserved (1.83±0.03 vs 1.83±0.09). (F) Total cation content of RBCs from control (blue, 139.4 mmol/lcw) and patient (red, 128.5 mmol/lcw) with addition of Na^+ and K^+ intracellular concentrations. (E-F) Averages +/- sem from n=3 independent experiments

Figure 2. Functional characterization of cation channel activity in D669Y Piezo1 RBCs.

(A-B) Monitoring of membrane potential using CCCP technique. (A) Control (blue) and patient (red) RBCs in a normal Ringer solution, followed by addition of the calcium ionophore A23187 (10µM). (B) Control (blue) and patient (red) RBCs in a LIS solution with continuous chloride conductance inhibition using 100µM NPPB, followed by addition of Ca^{2+} (1mM). A and B representative curves of 3 independent samples from 3 consultations over 2 years. (C) Fluorescence of Control (blue, n=34) and Patient (red, n=35) RBCs loaded with Fluo-4, before and 3min after addition of yoda1 (10µM). Insert shows together initial Ca^{2+} fluorescence at a magnified scale. ** indicates p<0.01, **** indicates p<0.0001. (D) Patch clamp whole-cell recording from control (blue) and patient (red) RBCs, stimulated from V_m=100 to V_m=-100mV by ramps of 500ms (black). (E) Corresponding whole-cell I/V curves from Control (blue circles, n=6) and Patient (red circles, n=7) RBCs. Patient RBCs show heterogeneous profile, with either cation current similar to control (pattern A, red triangles up, n=3) or spontaneous enhanced cation channel activity (pattern B, red squares, n=4).

Figure 1

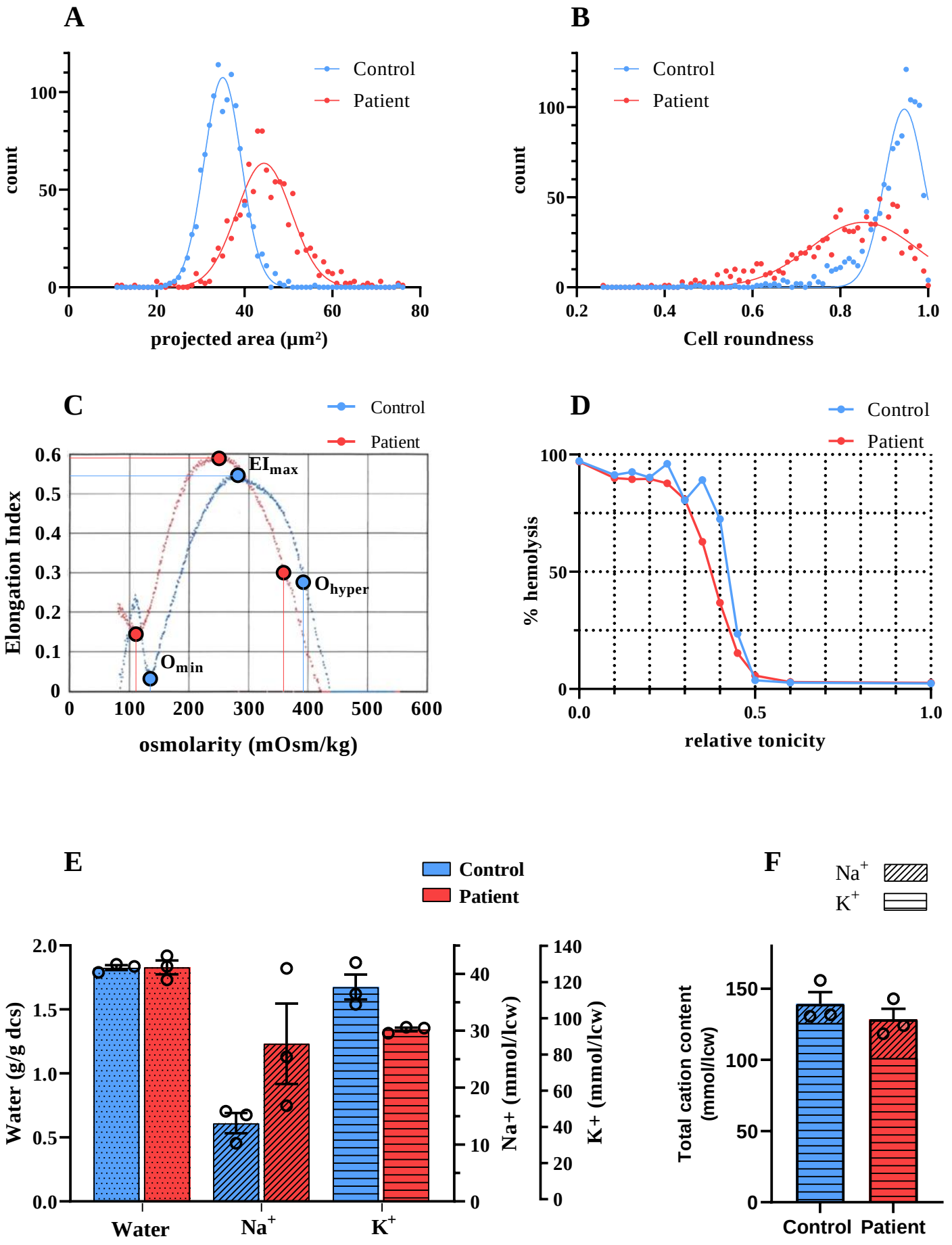
A
Control
Patient
count
projected area (µm²)
B
Control
Patient
count
Cell roundness
C
Control
Patient
Elongation Index
osmolarity (mOsm/kg)
D
Control
Patient
% hemolysis
relative tonicity
E
Control
Patient
Water (g/g dcs)
Na+ (mmol/lcw)
K+ (mmol/lcw)
Water
F
Total cation content (mmol/lcw)
Control
Patient

Figure 2

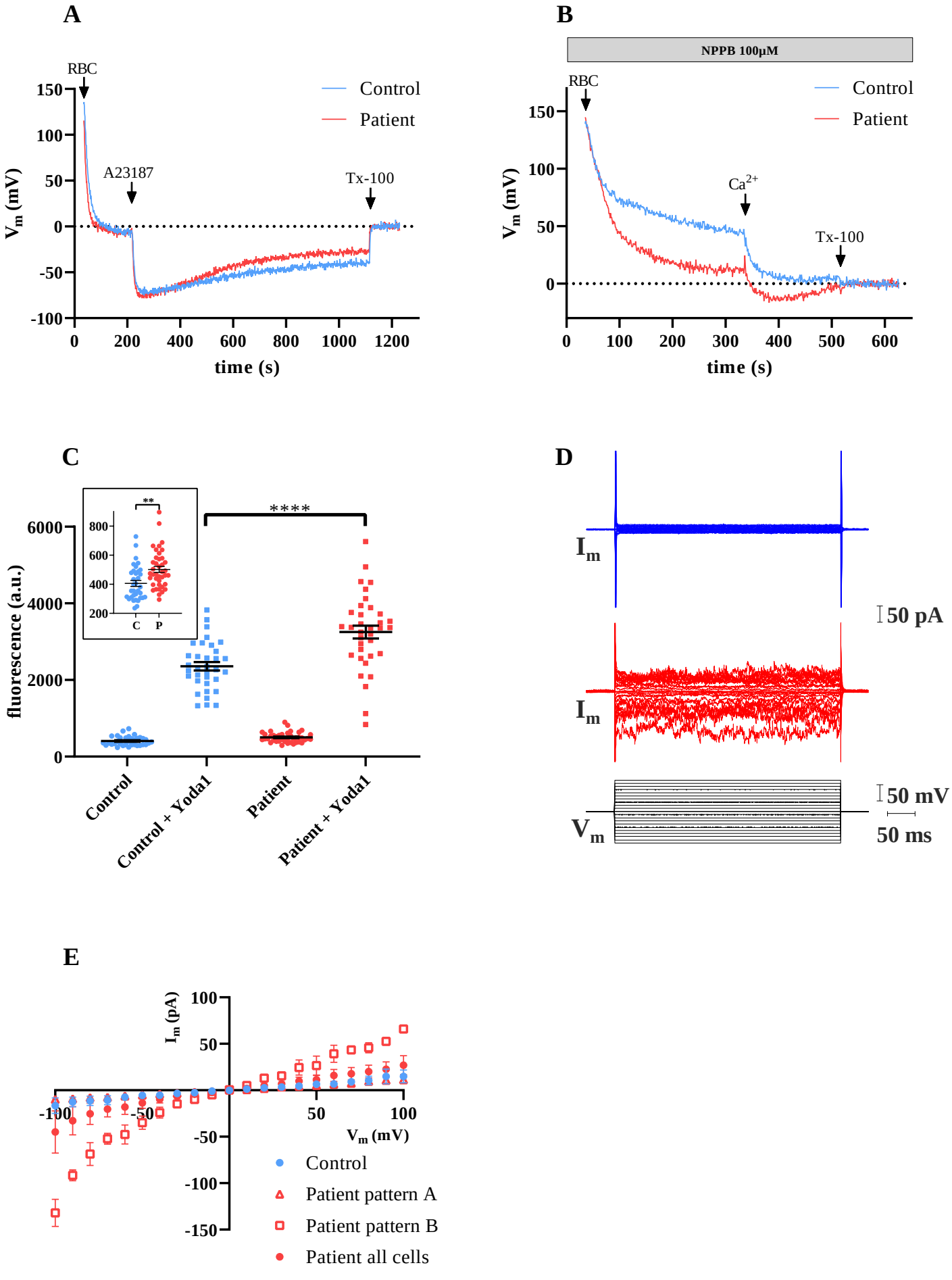
A
RBC
Control
Patient
A23187
Tx-100
V_m (mV)
time (s)
B
NPPB 100µM
RBC
Control
Patient
Ca^{2+}
Tx-100
V_m (mV)
time (s)
C
fluorescence (a.u.)
****
**
C
P
Control
Control + Yoda1
Patient
Patient + Yoda1
D
I_m
50 pA
I_m
V_m
50 mV
50 ms
E
I_m (pA)
V_m (mV)
Control
Patient pattern A
Patient pattern B
Patient all cells

Supplementary fig. 1

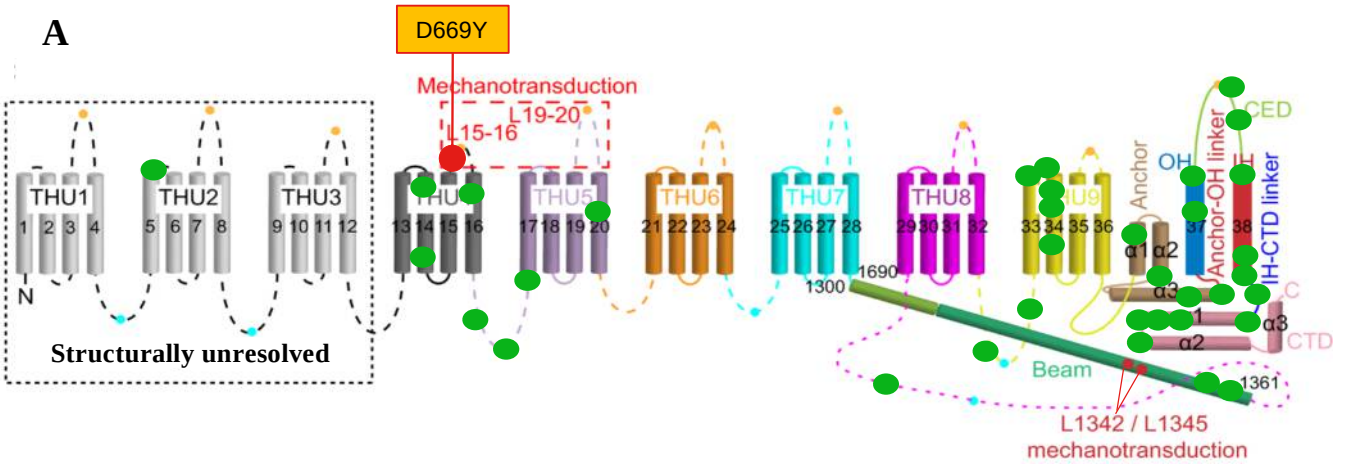

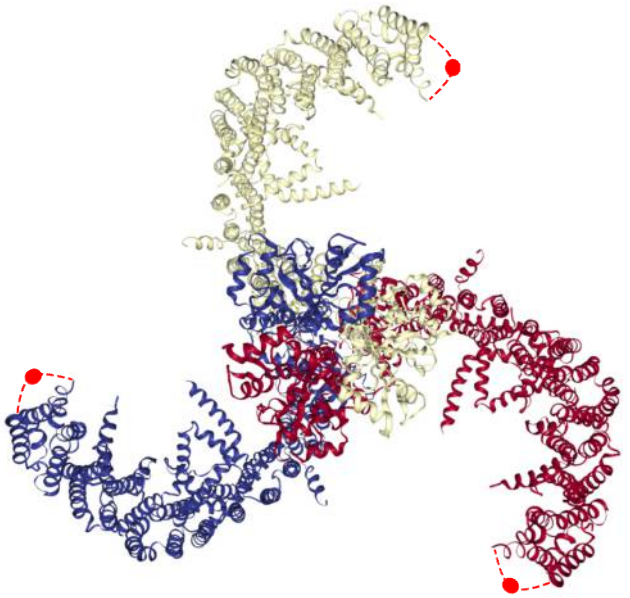

C

```
mPiezo1  LTGFTDEQLGDLGLEQFSVSE  685
hPiezo1  LTGFTDEQLGDLGLEQFSVSE  679
mPiezo2  MTGLKKEKLEDLGLKQFTVAE  790
hPiezo2  MTGLKKEKLEDLGLKQFTVAE  786
dPiezo   YLNVSATLQKDIGLKRYQTKD  693
```

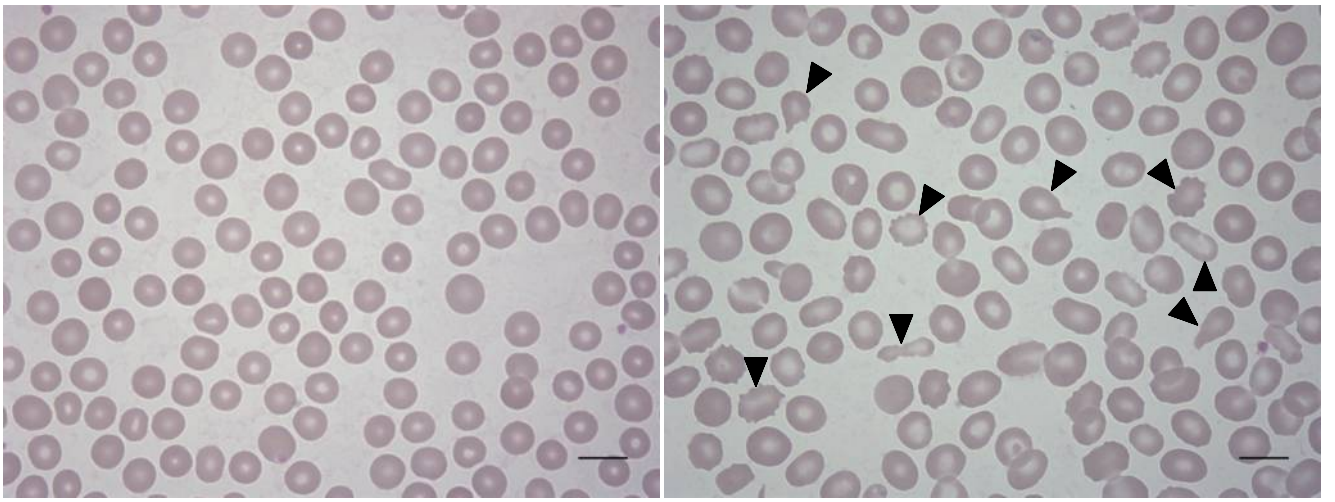

Supplementary Material

Characterization of Asp669Tyr Piezo1 cation channel activity in red blood cells: an unexpected phenotype

Laurent Pérès, David Monedero Alonso, Morgane Nudel, Martin Figeac, Judith Bruge, Shéhérazade Sebda, Véronique Picard, Wassim El Nemer, Claude Preudhomme, Christian Rose, Stéphane Egée, Guillaume Bouyer

Legend of Supplementary fig 1.

Localisation of D669 in Piezo1 protein and representative blood smears of D669Y RBCs. (A) Topology model for mPiezo1, modified from (1). The localization of D669Y mutation is indicated, as well as 36 other mutation sites (green dots) linked to HX families reported in (2). THU, Transmembrane Helical Units. (B) 3D structure of Piezo1 channel. Image from the RCSB PDB (rcsb.org) of PDB ID 5Z10 (3) . Red dot on an extracellular loop indicate localisation of the residue D669 in the three subunits constitutive of the channel. THU 1, 2 and 3 from the N-ter side are unresolved and thus not represented. (C) Sequence alignment of region of interest of mouse (m) and human (h) Piezo1 and Piezo2 and *Drosophila melanogaster* Piezo (dPiezo), showing the highly conserved motif containing D669 in human Piezo1, modified from (3). (D) Control (left) and patient (right) RBCs peripheral blood smears (100x objective), arrows indicate several aberrant shapes. Scale bar 10µm.

Description of results obtained with CCCP method (fig 2A-B)

The CCCP method allows live monitoring of membrane potential of a RBC suspension, via the recording of extracellular pH (see materials and methods below).

In Figure 2A, in a Normal Ringer solution, we injected control or D669Y Piezo1 RBCs. Rapidly for both cell types, the membrane potential stabilized to a value close to the theoretical membrane potential for RBCs (-12mV), indicating that this mutation does not alter chloride conductance or Band3 efficiency. We then challenged the membrane potential by addition of A23187, a Ca^{2+} ionophore that leads to a fast and maximal activation of the Gárdos channel.

Hyperpolarization peak (shift of membrane potential towards more negative values) reached the same amplitude in both cell types, leading to the conclusion that Gárdos channel activity is not affected by the mutation. The repolarization occurring after maximal hyperpolarization corresponds to a cation influx (Na^+, the only permeant cation in the extracellular medium) through another conductive pathway. This repolarization is accelerated in D669Y Piezo1 RBCs (fig. 2A), unveiling an increase in the activity of a cation channel, most likely Piezo1.

In figure 2B, to estimate the cationic channel activity, cells were challenged in a Low Ionic Strength (LIS) media that stimulates Non Selective Cation Channel (NSC) activity in human RBCs (4), in the presence of 100µM NPPB to inhibit chloride conductance. This condition proved valuable to detect Piezo1 gain-of-function (5). In D669Y Piezo1 RBCs, this NSC channel activity was enhanced compared to control RBCs (compare initial slope after cell injection). This slope corresponds to the efflux of cation through channel which tends to repolarize membrane potential towards initial resting membrane potential. Thus the repolarization speed reflects the strength of the ion current. Injection of Ca^{2+} confirmed previous observations regarding unaltered Gárdos channel function: hyperpolarizations after Ca^{2+} injection are similar for both type of cells.

Materials and Methods

Drugs and reagents

All salts were acquired from Sigma-Aldrich (Saint Quentin Fallavier, France) and are of analytical grade or better. A23187 (calcymicin; 5-(methylamino)-2-[[(2S,3R,5R,6S,8R,9R) -3,5,9-trimethyl-2-[(2S)-1 -oxo-1-(1H-pyrrol-2-yl)propan-2-yl] -1,7-dioxaspiro[5.5]undecan-8-yl]methyl] -1,3-benzoxazole-4-carboxylic acid), CCCP (carbonyl cyanide 3-chlorophenylhydrazone), NPPB (5-Nitro-2-(3-phenylpropylamino)benzoic acid), Triton™ X-100 (Tx-100) and Bovine Serum Albumin (BSA) were also purchased from Sigma-Aldrich. Yoda1 was purchased from Tocris Bioscience (Bio-Techne, Rennes, France).

Patient sampling and ethical statement

Patient and Control blood were withdrawn upon written informed consent, in accordance with the Helsinki Declaration of 1975, as revised in 2008. Blood was shipped overnight in heparinized tubes at 4°C and processed. This work has been approved by the institutional CNRS

Bioethics committee (INSB) and by the French Ministry for Research (declaration DC-2019-3842).

Molecular analysis

DNA sample from the patient and his parents were analysed by whole exome sequencing using the AmpliSeq Technologies and ion-torrent HiQ sequencing (Thermo Fisher Scientific). Each sample leads to the preparation of two libraries with different indexes in order to eliminate PCR and sequencing errors. Each individual was sequenced with at least 65 000 000 reads of approximately 183bp. Raw data were analysed with the Torrent Suite v5.0.4 (Thermo Fisher Scientific) to give variant in VCF format (TSVC germline pipeline with low stringency parameters). More than 92% of the AmpliSeq Exome (35Mb) was sequenced with at least 20x depth. Then variant for each individual were pooled together, annotated with VEP v83 and filtered for quality, absence in international databases and de novo hypothesis. The *de novo* hypothesis identified only one coding variant, the Piezo1 NM_001142864.2:c.2005G>T variant. The variant was predicted to be deleterious by SIFT and PolyPhen.

Cell morphology analysis

Smears were prepared from Patient and Control blood shipped to our lab within 24h at 4°C, fixed with methanol and stained with freshly prepared Giemsa (10%, 15min) (Sigma-Aldrich). Pictures were taken under a microscope with a 100x objective and morphology analyses were performed using Fiji (6) .

Osmoscan

Osmotic gradient ektacytometry was performed on EDTA blood sample after 24 hours/4°C sending using a Technicon® ektacytometer as previously described (7). In brief, red cells were continuously mixed with a 4% polyvinylpyrrolidone solution of gradually increasing osmolality (from 60 to 450 mOsm), and the deformability index was recorded as a function of osmolality at a constant applied shear stress of 170 dynes/ cm^2.

Osmotic fragility curves

OFCs are obtained by rapidly diluting RBC samples into relatively large volumes of media with progressively reduced relative tonicity. Briefly, 10µl of donor whole blood was added to 500µl of solutions of various relative tonicity prepared with distilled water (0=100% water, 1=290 mOsmol/kg). Unlysed cells were then spun down, and the fraction of cells lysed in each of the hypotonic conditions is estimated from the fraction of haemoglobin (Hb) released to the supernatant by reading the absorbance at 540nm.

Cell water and Na^+/K^+ content

0.5 ml aliquots of the cell suspension were distributed in polyethylene micro test tubes and centrifuged at 20 000×g for 10 min at 4 °C. After centrifugation the packed cell mass was separated from the supernatant by slicing the tube with a razor blade below the top of the red cell column. **Water content:** After weighing, the packed cells were dried to constant weight for at least 24 h at 90 °C and re-weighed, and the ratio wet weight /dry weight calculated. **Na^+ and K^+ content:** Packed cells within the sliced tube were lysed in 1 ml MilliQ water. Proteins were denatured to ease separation by addition of 231.9 µM of perchloric acid. The tubes were spun at 16 900 g for 7.5 min at 4 °C and the supernatant passed onto sample tubes and diluted 10 times with milliQ water. Ionic content was measured using a flame photometer (PFP7, Jenway). The amounts Na^+ or K^+ measured are reported as mmol/liter cell water.

Membrane Potential recordings

The CCCP method was used for the monitoring of membrane potential evolution (8,9) . When erythrocytes are suspended in nominally buffer-free solution in the presence of the protonophore CCCP (10µM), changes in extracellular pH reflect membrane potential changes, since protons are kept at equilibrium across the membrane. The membrane potential can thus be estimated from:

$$V_M = -61.51\,mV \cdot (pH_o - pH_i)$$

Due to the high red cell buffering capacity, the intracellular pH remains constant (at about 7.2) throughout an experiment and can be estimated as the pH of the solution after lysis with Triton™ X-100 at the end of the experiment.

Solutions:

- Normal Ringer: 154 mM NaCl, 2 mM KCl (nominal Ca2+ content estimated at 4µM)

- Low Ionic Strength solution: 264 mM sucrose, 2 mM KCl (nominal Ca2+ content estimated at 4µM)

Calcium content observations

Calcium content of live erythrocytes was monitored using Fluo-4 fluorescence. Briefly, 50µl whole blood was first washed twice in a Normal Extra-Cellular Medium (NECM-BSA) (pH7.4) containing 137 mM NaCl, 3.5 mM KCl, 1mM $CaCl_2$, 1 mM $MgCl_2$, 10 mM Hepes, 10 mM glucose supplemented with 0.05% Bovine Serum Albumin. RBCs were then loaded with 5µM Fluo-4AM (ThermoFisher) in NECM-BSA for 1h30 at room temperature. After loading, cells were washed 4 times with NECM-BSA to remove excess Fluo-4-AM, and were imaged using a confocal microscope LEICA SP5 microscope (Merimage platform, Station Biologique, Roscoff, France).

Patch clamp recordings

Patch clamp experiments were performed at room temperature using the whole cell configuration. Pipettes were prepared using a DMZ Universal Puller (Zeitz Instruments, Germany) from borosilicate glass capillaries (GC150F-10, Harvard apparatus, UK), resulting in a pipette resistance of 10-15 MΩ. Patch clamp solutions were : Pipette 145 mM KCl, 1.85 mM $CaCl_2$, 1.2 mM $MgCl_2$, 5 mM EGTA, 10 mM Hepes, 10 mM, pH 7.2; Bath 145 mM NaCl, 5 mM KCl, 1 mM $CaCl_2$, 1 mM $MgCl_2$, 10 mM Hepes, 10 mM glucose, pH 7.4. When the seal resistance reached 4-20 GΩ, whole cell configuration was obtained by a brief electrical pulse (zap) and was assessed by development of small capacitance transient currents and reduction of access resistance. Whole cell current were recorded using a RK400 (Biologic, France) amplifier, with voltage command protocols and current analysis performed with WinWCP4.7 software (J. Dempster, Strathclyde University, UK). Currents were elicited by generating a series of membrane potentials from +100 to -100 mV in -10 mV steps for 500 ms, from a holding potential of 0 mV.

Statistical analysis

Differences between samples was assessed by using non-parametric Mann-Whitney test.

Supplementary material references

1. Zhao Q, Zhou H, Li X, Xiao B. The mechanosensitive Piezo1 channel: a three-bladed propeller-like structure and a lever-like mechanogating mechanism. FEBS J. 2019;286(13):2461‑70.

2. Picard V, Guitton C, Thuret I, Rose C, Bendelac L, Ghazal K, et al. Clinical and biological features in PIEZO1-hereditary xerocytosis and Gardos-channelopathy: A retrospective series of 126 patients. Haematologica. 2019;haematol.2018.205328.

3. Zhao Q, Zhou H, Chi S, Wang Y, Wang J, Geng J, et al. Structure and mechanogating mechanism of the Piezo1 channel. Nature. 2018;554:487.

4. Moersdorf D, Egee S, Hahn C, Hanf B, Ellory C, Thomas S, et al. Transmembrane potential of red blood cells under low ionic strength conditions. Cell Physiol Biochem. 2013;31(6):875‑82.

5. Filser M, Giansily-Blaizot M, Grenier M, Monedero Alonso D, Bouyer G, Peres L, et al. Increased incidence of germline PIEZO1 mutations in individuals with idiopathic erythrocytosis. Blood [Internet]. 2020;(blood.2020008424). https://doi.org/10.1182/blood.2020008424

6. Schindelin J, Arganda-Carreras I, Frise E, Kaynig V, Longair M, Pietzsch T, et al. Fiji: an open-source platform for biological-image analysis. Nat Methods. 1 juill 2012;9(7):676‑82.

7. Cynober T, Mohandas N, Tchernia G. Red cell abnormalities in hereditary spherocytosis: Relevance to diagnosis and understanding of the variable expression of clinical severity. J Lab Clin Med. 1 sept 1996;128(3):259‑69.

8. Macey RI, Adorante JS, Orme FW. Erythrocyte membrane potentials determined by hydrogen ion distribution. Biochim Biophys Acta. 22 sept 1978;512(2):284‑95.

9. Bennekou P, Christophersen P. Flux ratio of valinomycin-mediated K+ fluxes across the human red cell membrane in the presence of the protonophore CCCP. J Membr Biol. 1986;93(3):221‑7.